Tikrit Journal of Pure Science Vol. 29 (2) 2024

TJPS

https://doi.org/10.25130/tjps.v29i2.1521

IASJ

المجلات الاكاديمية العراقية

Tikrit Journal of Pure Science

ISSN: 1813 – 1662 (Print) --- E-ISSN: 2415 – 1726 (Online)

Journal Homepage: http://tjps.tu.edu.iq/index.php/j

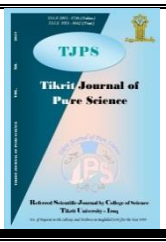

Study the Effect of Copper Oxide Nanorods Enhanced by Silver Nanoparticles on the Highly Sensitive Gas Sensor

Shahad Ahmed Dheyab , N. K. Hassan

Department of Physics , College of Education for Pure Sciences , Tikrit University , Tikrit , Iraq.

ARTICLE INFO.

Article history:

-Received: 19 / 8 / 2023

-Received in revised form: 18/ 9 / 2023

-Accepted: 23 / 9 / 2023

-Final Proofreading: 17 / 12 / 2023

-Available online: 25 / 4 / 2024

Keywords: CuO, AgNPs growth on CuO, Nanorods morphology, NH_3 sensitivity

Corresponding Author:

Name: N. K. Hassan

E-mail: nadimkh4@tu.edu.iq

Tel: 00964-77212166

ABSTRACT

In this paper, ammonia (NH_3) gas sensitivity was enhanced by the development of highly dense copper oxide (CuO) nanorods on glass substrates. The layer of copper (Cu) was deposited using a vacuum thermal evaporation method. The grown layer of Cu was sequentially inserted into an oxidation furnace at (400 °C) for (120 min) under atmospheric pressure to produce copper oxide (CuO) nanorods. Silver (Ag) nanoparticles- deposited copper oxide nanoparticles were successfully enhanced via a photo assisted spray pyrolysis technique. A metal-semiconductor-metal (MSM) NH_3 gas sensor with aluminum (Al) contact electrodes was fabricated on CuO nanorods. The structure of the crystal as well as the morphology of the CuO nanorods were evaluated with field-emission scanning electron microscopy (FE-SEM), X-ray diffraction, and UV-visible spectroscopy respectively. In order to create a high-performing MSM NH_3 gas sensor, silver nanoparticles (NPs) were sprayed by the photo-assisted spray pyrolysis technique on the CuO nanorods, which are produced via the vacuum thermal evaporation method. The results showed that the modified CuO nanorods by Ag nanoparticles demonstrated great sensitivity to NH_3 gas might be much improved, and the sensitivity rises from (376.4 to 700 %) , fast response and recovery times about (10.4 and 9.5 s) respectively to NH_3 gas.

دراسة تأثير قضبان أوكسيد النحاس النانوية المعززة بجسيمات الفضة النانوية على المتحسس الغازي عالي الحساسية

شهد احمد ذياب ، نديم خالد حسن

قسم الفيزياء ، كلية التربية للعلوم الصرفة ، جامعة تكريت ، تكريت ، العراق

الملخص

تم في هذا البحث، تم تعزيز حساسية غاز الأمونيا (NH_3) من خلال ترسيب قضبان نانوية من أكسيد النحاس عالي الكثافة (CuO) على قواعد زجاجية. تم ترسيب طبقة النحاس (Cu) باستخدام طريقة التبخر الحراري في الفراغ. تم نقل الطبقة المزروعة من النحاس على التوالي إلى فرن للأكسدة عند (400 درجة مئوية) لمدة (120 دقيقة) تحت الضغط الجوي لإنتاج قضبان أكسيد النحاس (CuO) النانوية. تم تعزيز خصائص جسيمات اوكسيد النحاس النانوية المرسبة بترسيب جسيمات الفضة النانوية عليها بنجاح عبر تقنية الانحلال الحراري بالرش بمساعدة الضوء. تم تصنيع متحسس معدن–شبه موصل–معدن MSM لغاز NH_3 مع أقطاب اتصال Al على قضبان CuO النانوية. تم تحليل مورفولوجيا النمو والتركيب البلوري لقضبان(CuO) النانوية باستخدام المجهر الإلكتروني الماسح ذو انبعاث المجال (FE-SEM) وحيود الأشعة السينية والتحليل

Tikrit Journal of Pure Science Vol. 29 (2) 2024

TJPS

https://doi.org/10.25130/tjps.v29i2.1521

الطيفي للأشعة فوق البنفسجية المرئية على التوالي. من أجل إنشاء متحسس غاز NH_3 MSM عالي الأداء، تم ترسيب جسيمات الفضة النانوية (Ag- NPs) بطريقة الرش الحراري المستحث بالضوء على سطح القضبان النانوية المنتجة بالتبخير الحراري الفراغي لـ CuO المرسب على الركيزة الزجاجية. وجدنا من النتائج أن قضبان CuO المعدلة بالجسيمات النانوية للفضة Ag أظهرت تحسن حساسية غاز الامونيا بصورة كبيرة حيث وجدنا ان الحساسية ارتفعت من (376.4 إلى 700 ٪)، مع نقصان في زمني الاستجابة والاسترداد حوالي (10.4 و 9.5 ثانية) على التوالي إلى غاز NH_3.

1. Introduction

Ammonia (NH_3) is a dangerous and toxic gas that is extensively used in a variety of industrial processes, including those in the food, chemical, textile, fertilizer, and automotive sectors [1]. Ammonia leaks seriously damage the environment, creating dangers for human life. Currently, one of the most popular commercial sensing element materials is copper oxide (CuO). A variety of CuO nanostructures with high surface-to-volume ratios have been grown as a result of countless in-depth studies because of the complementary benefits of CuO nanomaterials with well-defined morphological structures. These structures are crucial for the production of gas sensors because they have high gas sensitivity and quick response and recovery times [2]. Among these various morphologies, the crystal-like CuO nanostructure is a p-type metal oxide semiconductor (MOS) material with a narrow indirect band gap of (1.2-1.8 eV) [2-4] and exceeds (2 eV) direct band gap [5,6] have received a lot of attention recently due to their distinctive shape and structure, which produce exceptional physical and electrical properties make it is a key component in optoelectronics and sensing [3,7]. Due to its high potential as a sensing material, CuO nanostructure has received extensive attention for sensing material applications [4]. P-type metal oxide gas sensor has a few benefits over the n-type metal oxide gas sensor. The identical morphological arrangements of both sensor materials [8]. A p-type oxide semiconductor gas sensor responded to some gases in a manner that was equal to the square root of an n-type oxide semiconductor sensor [9]. Various synthetic techniques have been reported in recent years for the production of CuO nanoparticles; wet chemical methods, low-temperature solid-phase processes, oxidation reactions caused by heating copper substrates in the air, or electrodeposition [10-13].

Numerous researchers have primarily concentrated on the growth of diverse nanostructured CuO materials using various growth techniques and explored the properties of these materials for gas sensing, such as nanowires, nanorods, nanotubes, nanoflowers, and nanoparticles [14-24]. This work, focus on the electrical parameters of the self-powered UV MSM detector with the structure of the Ag NPs/CuO nanorods/Galss, fabricated via photo-deposition method, despite the fact that there have been numerous studies examining the effects of adding the Ag NPs on the surface of metal oxides [25].

In this work, vacuum thermal evaporation was used to deposit a two layers of CuO on glass to grow copper oxide nanorods (CuO NRs), where Cu deposited and oxidize under heat treatment for two times via thermal oxidation and then to cool down. Photo-assisted spray pyrolysis was used to coat nanorods with silver nanoparticles (Ag), and aluminum (Al) was deposited as metal electrodes. This was done to make a NH_3 gas sensor. Before looking at how sensitive NH_3 is, the shape, structure, and optical properties of a rod-like CuO nanostructure were also looked at.

2. Experimental Detail

Glass substrates were immersed in the mixture of acetone and ethanol rinsed in deionized water after being heated for (10 min). After cleaning the glass substrates were placed over the substrate holder at a distance of (20 cm) away from the tungsten boat contains high-purity copper powder (1 g, 99.999%, Sigma-Aldrich) (Cu) was thermally evaporated on the glass in vacuum thermal evaporator, a copper (Cu) layer was deposited on the glass surface the resulting sample (Cu/glass) was orderly introduced inside a thermal furnace at (400 °C) under ambient gas for (120 min), and then the temperature of the furnace was lowered to ambient to produce copper oxide (CuO) thin film, this thin film was used as a substrate and then the process was repeated by precipitating copper for the second time and then oxidizing it under a temperature of (400 °C) to produce copper oxide nanorods.

Silver (Ag) nanoparticles are deposited by photo (365 nm wavelength) assisted spray pyrolysis in air environment onto the CuO nanorods as substrate. The initial solution is prepared from solid silver nitrate ($AgNO_3$) (99.9 % purity with a molar mass of 169.87 g/mol) diluted in distilled water the molarity (M) was (0.009 M), this solution is dissolved in a (1M) sodium hydroxide solution that has been dissolved in (10 ml) of distilled water. The silver deposition process was performed under UV- light (365 nm wavelength) with a spray rate of about (5 ml/min) on the CuO substrates. In order to produce homogenous films with good adhesion of Ag on CuO nanorods, CuO substrates were heated at a temperature of (70 °C) in atmospheric pressure.

The morphology and crystallinity of the CuO nanorods were characterized using field-emission scanning electron microscopy (FESEM, NOVA NANOSEM 450, USA) and X-ray diffraction (XRD) by X-ray diffractometer system type of (Philips PW

https://doi.org/10.25130/tjps.v29i2.1521

1710, USA), the source of radiation was Cu (kα) and (λ = 1.5406 Å) respectively.

While the optical properties of the deposited films were recorded with UV–Vis (Shimadzu, UV-3600) spectrometers at room temperature. Two interdigitated electrodes with four fingers each make up the MSM gas sensor. Each finger measures (230 m) in width, (3.3 mm) in length, and (400 µm) separates each finger. Utilizing a metal mask created using the contact structure's pattern, aluminum (Al) contacts were formed using vacuum thermal evaporation [26]. Gas sensor performance measurement set-up is shown in Fig. (1). The change in sensor resistance when exposed to NH_3 gas is taken. CuO sensor was placed inside the chamber (Fig. 1), later the desired gas (NH_3) with concentration of (17.25) ppm was injected.

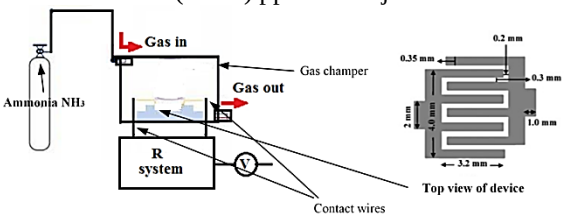

Fig. 1: Schematic illustration of measurement set-up

3. Results and Discussion

3.1 Characterization of the CuO nanorods

Figures (2 a and b) show the typical FESEM images of the CuO nanorods grown on glass substrates. It can be seen that the grown CuO consists of well-defined nanorod structures composed of regular cubic structures. A highly dense rod shape of CuO was successfully obtained, with an average length of (200 nm). The importance of the first thin layer of CuO, which acts as a buffer layer, is to prevent the crystal mismatch usually seen when CuO is directly deposited on glass substrates. Generally, the buffer layer acts as an intermediate layer between the amorphous substrate and thin film. The reasons why the buffer layer plays an important role are as follows: Amorphous substrates are not well-defined crystals, which causes difficulty in the growth of thin films and obtaining a well-defined structure.

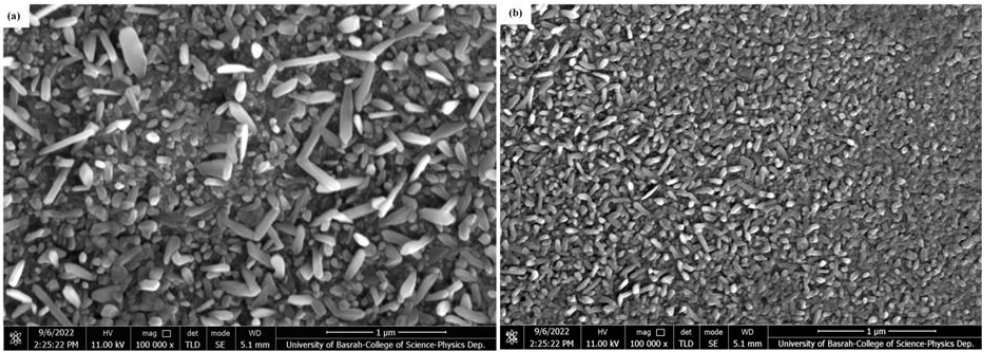

Fig. 2: FESEM images: (a) CuO nanorods deposited on CuO thin layer, (b) CuO nanorods with Ag nanoparticles

Therefore, in order to overcome the crystal mismatch and begin nucleation and growth, the lattice constants of the new material to be deposited and the substrate should be the same. Nucleation, growth, enhanced compatibility, adhesion, in addition to improving the surface shape and crystalline control. The substrate and the substance to be deposited must match in order to achieve each of these. After the heating procedure, nanorods of copper oxide layer are generated between the CuO layer and the glass substrate, forming a CuO layer between the higher CuO layer and lower glass substrate. The following mechanisms of nanonrods production are suggested and explained: Nothing can reduce the downward diffusion of oxygen to the copper oxide substrate or the reaction between the second layer of Cu atoms and oxygen in the air for a glass-coated copper that has been annealed at (400 ^{o}C). As a result, the surface of the first layer of CuO is swiftly oxidized, and CuO is created by the second oxidation of Cu_2O in the manner described below [25]:

$$4Cu + O_2 \longrightarrow 2Cu_2O \quad \ldots.(1)$$

$$2Cu_2O + O_2 \longrightarrow 4CuO \quad \ldots(2)$$

From the Fig. (2 a and b) it can be seen that the annealing temperature can significantly influence the size and shape of CuO nanorods. Annealing temperatures can increase the diffusion of atoms or molecules and enhance the growth of nanoparticles. Higher annealing temperatures can result in larger particle sizes. On the other hand, lower annealing temperatures may decrease the diffusion, leading to smaller particle sizes [25]. Therefore, by controlling the annealing temperature, it can help to obtain a size that is effective in sensors.

The crystal structure of nanorods is greatly affected by depositing Ag nanoparticles. Fig. (2 b) shows that the spaces between the CuO nanorods are completely

https://doi.org/10.25130/tjps.v29i2.1521

filled with Ag nanoparticles. The annealing can influence the preferential growth directions of nanorods, resulting in uniform shapes and a high density of CuO nanorods. One possible method for producing CuO on the substrate's surface is the oxidation of the Cu substrate by oxygen atoms from the air that have spread downward. Due to the continual diffusion of oxygen atoms into the deeper region of the substrate, the oxide's thickness grows as the heating time increases. Copper oxide is made in the deeper, oxygen-free zone. The surface area of the copper oxide is then turned into CuO nanorods using the CuO crystals made in the first layer.

Figure (3) depicts the XRD patterns of crystal structure of CuO nanorods annealed at temperatures of (400 ^{o}C) and Ag-CuO nanorods. It can be observed that the X-ray pattern confirms that the samples obtained are crystalline and have the monoclinic structure of CuO. The decomposition of CuO nanorods like is believed to carry out in two steps: Cu first decomposes to Cu_2O and O_2, followed by the decomposition of Cu_2O to CuO and O_2 at a higher temperature. The peaks positions and relative intensities of the diffraction peaks of (32.5º, 35.5º, and 38.9º) correspond to the lattice plane of (110), (111) and (002) respectively reflections, in agreement with JCPDS data for CuO (JCPDS: card no. 48-1548) [27-29]. Therefore, the result here confirmed the evaporated films are CuO. The appearance of Ag peaks in the XRD pattern of CuO can be attributed to small amounts of Ag impurities and, the possibility of some Ag forming along with CuO. From the figure, it is noticed that the appearance of high peaks was at Fig. (3 a), indicates the purity of this thin film.

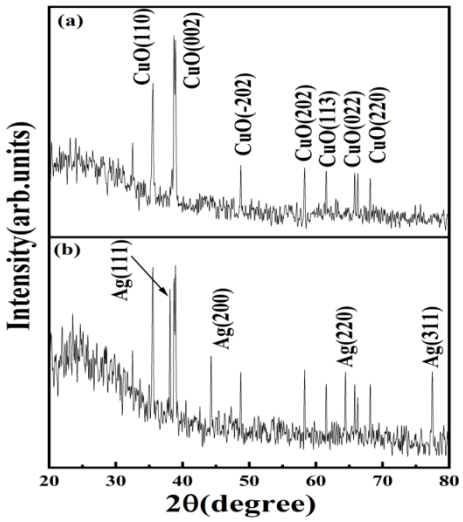

Fig. 3: XRD spectrum: (a) CuO nanorods deposited on CuO thin layer, (b) CuO nanorods with Ag nanoparticles.

No peaks of Cu metal are observed in the XRD patterns, indicating that phase-pure CuO is readily obtained. It can be clearly observed that the Ag peaks with different intensities of the peaks in the XRD spectra of sample (Fig. 3 b) revealed that the film is mainly composed of CuO and contains a small amount of Ag. According to the XRD data, CuO nanorods and Ag-CuO nanorods were the primary phases of nanoscale CuO nanotubes formed on pure CuO/glass substrates after vacuum thermal evaporation that was followed by oxidation.

Figure (4) shows the linear relationship between the $(\alpha h\nu)^2$ and photon energy ($h\nu$) was obtained by plotting $(\alpha h\nu)^2$ against ($h\nu$) to determine the value of the optical energy gap at (α = 0), where α is the absorption coefficient and $h\nu$ is the photon energy. The energy band gap of CuO rods is found to be (1.79 eV) for the CuO nanorods sample annealed at (400 and 1.89 eV) for the same sample after Ag nanoparticles deposited, these are greater than of the bulk CuO band gap. The observed deviation to blue shift in the value of the energy gap occurred due to the quantum confinement effect resulting from the reduction in the size and dimensional structure of the nanoparticles and the existence of an amorphous phase in films [5,6]. The change in energy gap values after Ag nanoparticles deposition could be because both the electrical structure of CuO nanorods and that of Ag nanoparticles can be altered by these actions. Quantum confinement might change the materials' internal energy levels, which might have an impact on the energy gap. CuO nanorods sample annealed at (400 ^{o}C) energy gap (Fig. 4 a) increases in its value. These values match to the energy gaps of direct gap of p-type CuO [30,31]. Energy gap values showing that a direct allowed transition was the cause of the absorption edge [32]. It is clear that the direct band gap increases with decreasing particle size [33]. At the interface between the Ag nanoparticles and the CuO nanotubes, the addition of Ag nanoparticles can alter or produce new surface states. In addition Ag nanoparticles can produce plasmonic phenomena, in which the collective oscillations of the Ag nanoparticles' electrons take place. The CuO nanorods can pair with these plasmonic phenomena, which will change the energy gap.

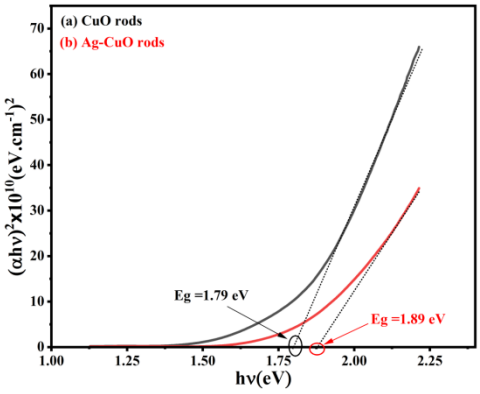

Fig. 4: Tauc's plot: (a) CuO nano-rods deposited on CuO thin layer, (b) CuO nanorods with Ag nanoparticles

3.2 Characteristics of the Nanorods -like CuO MSM NH_3 sensor

https://doi.org/10.25130/tjps.v29i2.1521

The schematic of the CuO NRs MSM NH_3 sensor, as well as the Al finger contacts deposited on top of the CuO nanorods is shown in Fig. (1). To describe a NH_3 sensor performance characteristics, electrical responses of the gas sensors fabricated from Al/CuO NRs /Al and Al/ Ag-CuO NRs /Al were investigated at room temperature, and (17.25 ppm) NH_3 gas. Figure (5) Shows the electrical responses of rod-like CuO as a function of time. The enlarged parts of our recorded data have been drawn in Fig. (5 a and b) measured at a NH_3 concentration of (17.25 ppm) in case of gas input and gas stop. The gas response, response time, and recovery time were used to describe the gas-sensing performances. This formula was used to determine the gas response [34].

$$R_{response}\% = \left|\frac{R_{air}-R_{gas}}{R_{air}}\right| x100 \ldots\ldots (3)$$

The sensor's reaction grew linearly as the quantity of ammonia gas increased. When exposed to fresh air, the response immediately returns to the initial value; this shows that the Al/CuO/Al sensor has strong repeatability and reproducibility. The response and recovery times of a gas sensor are another crucial fundamental element. For real-time use in practical applications, a sensor with quick reaction and recovery is required. Response time was found to be (12.4 s) for (17.25 ppm) ammonia gas, and recovery time is (6.7 s), as shown in Table (1) for the sensor based on CuO nanorods.

Table 1: Variation of Sensitivity, Response and Recovery time of gas sensor with based on CuO without and with Ag nanoparticles

Sample annealing temperature	Sensitivity	Response time(S)	Recovery time(S)
Al/ CuO/Al	376.4	12.4	6.7
Al/Ag-CuO/Al	700.7	10.7	9.7

The reactions at the CuO nanorods surface and the diffusion are the basis for the basic operation of NH_3 gas sensor. Surface polarity and enhanced oxygen adsorption at the CuO surface upon exposure to ammonia gas at room temperature. Based on the energy gap values obtained, during thermal treatment p-type CuO could be formed [35, 36], which was confirmed by the behavior of the sensor where there was a change in the resistance values of the sensor with its with exposure to ammonia gas [34]. The sensor response to (17.25 ppm) NH_3 was measured, as shown in Fig. (5). The CuO gas sensor's related dynamic response characteristics to (17.25 ppm) NH_3 at various times. The real-time on/off switching was measured by exposing the NH_3 gas. While exposed to NH_3 gas, the measured current developed rapidly before decreasing when there is no gas flow. The response and decay times for the sensor CuO they were calculated.

CuO's resistance decreases as a result of the removal of electrons by surface oxygen species and the formation of holes in the material. Upon exposure to NH_3, ammonia reacts with CuO, it can act as a reducing agent, and possible reduction reaction path at the CuO surface can be given as follows [34, 37, 38],

$$NH_3(gas) \leftrightarrow NH_3(ads) \ldots . (4)$$
$$3O_2^- + 4NH_3 \leftrightarrow 2N_2 + 6H_2O + 3e^- \ldots . (5)$$
$$3O^- + 2NH_3 \leftrightarrow N_2 + 3H_2O + 3e^- \ldots . (6)$$
$$3O^{2-} + 2NH_3 \leftrightarrow N_2 + 3H_2O + 6e^- \ldots . (7)$$

Based on their reactivity with reducing gas molecules and the adsorption/desorption of those molecules, CuO sensors' ability to detect the presence of gas as an explanation for a change in sensor resistance. In the initial stages, oxygen molecules get absorbed through the CuO sensor when exposed to air, atmosphere, and oxygen ionic species (O^{2-}, O^-, and O^{2-}) are formed through capturing one electron from the CuO surface.

Consequently, there is a decrease in electrical resistance due to an increase in hole concentration. When exposed to reducing gases such as ammonia molecules, ionic oxygen species (on the surface of CuO) interact with these molecules, causing many electrons to be released back into the CuO conduction band. Recombining these electrons with the existing holes raises the electrical resistance of the CuO sensor. As a result, the electrical resistance of the sensor changes in a manner that is proportionate to the presence of ammonia gas.

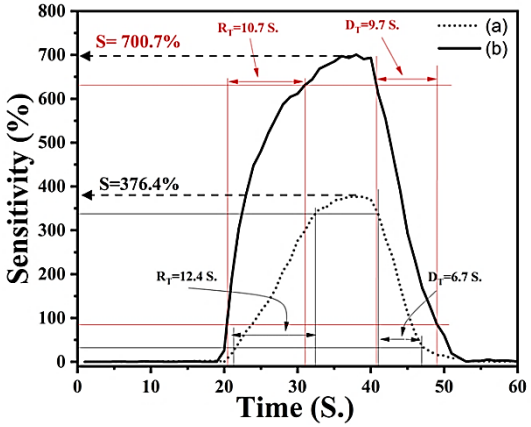

Fig. 5: NH_3 sensing responses: (a) CuO nano-rods deposited on CuO thin layer, (b) CuO nano-rods with Ag nanoparticles

When CuO nanorods surfaces consist of a large number of Ag nanoparticles, contact at their boundaries lowers the Schottky barrier height at the interface of adjacent grains. This is brought on by charge trapping at the interface and governs the electrical behavior. The conductivity is determined based on the height of this barrier. Charge trapping at the interface is what caused this process. Majority of carriers can be caught in trap states that are present at these interfaces. As a result, the band bends, creating a barrier at the interface. The conductivity of this barrier is regulated by its height [39]. It is evident that the relationship between the change in conductance and the change in barrier height and the temperature. When determining the sensitivity of CuO gas sensors,

https://doi.org/10.25130/tjps.v29i2.1521

grain boundaries are a key factor through its effect on the value of the height of the Schottky potential barrier. Gas molecules react and adsorb on the surface of CuO particles as part of the sensing mechanism. The electrical characteristics (Fig. 5) of the sensor alter as a result of the gas molecules diffusing across the grain boundaries and interacting with the CuO surface. From the results that we obtained, it was shown that the annealing temperature has a large effect on the size of the grains and therefore on the sensor. Our results showed that with the wide spread of the grains on the substrate, the values of the grain boundaries decreased, thus decreasing the sensitivity of the sensor, and the values of response and recovery times decreased, as shown in Table 1.

4. Conclusions

CuO nanorods were grown on CuO nanoparticles or glass substrates by oxidizing at (400 °C) annealing temperatures two layers of CuO that were deposited on glass using the vacuum thermal evaporation deposition technique. The morphology of the sample showed that the grown CuO was nanorods. The Ag nanoparticles were deposited by spray pyrolysis on CuO nanorods. The results demonstrate that high-quality CuO nanorods may be produced via affordable thermal deposition by appropriately regulating the lattice mismatch between substrate and deposited film by choosing a layer that acts as a buffering layer between the substrate and the layer that will be deposited. To enhance NH_3 sensor performance, the spaces between CuO nanorods are coated with Ag nanoparticles.

The suggested NH_3 sensor has exhibited both a fast response time and recovery time of less than (10.7 and 9.7 s) respectively, a wide range of detection of NH_3 with a sensitivity of (700.7 %).

References

[1] M. Poloju, N. Jayababu, M.V. Ramana Reddy, Improved gas sensing performance of Al doped ZnO/CuO nanocomposite based ammonia gas sensor, Materials Science and Engineering: B, 227 (2018) 61-67.

[2] L. Hou, C. Zhang, L. Li, C. Du, X. Li, X.F. Kang, W. Chen, CO gas sensors based on p-type CuO nanotubes and CuO nanocubes: Morphology and surface structure effects on the sensing performance, Talanta, 188 (2018) 41-49.

[3] D. Wu, Q. Zhang, M. Tao, LSDA+Ustudy of cupric oxide: Electronic structure and native point defects, Physical Review B, 73 (2006).

[4] N. Duc Hoa, N. Van Quy, M. Anh Tuan, N. Van Hieu, Facile synthesis of p-type semiconducting cupric oxide nanowires and their gas-sensing properties, Physica E: Low-dimensional Systems and Nanostructures, 42 (2009) 146-149.

[5] J. Koshy, M.S. Samuel, A. Chandran, K.C. George, P. Predeep, M. Thakur, M.K.R. Varma, Optical Properties of CuO Nanoparticles, in, 2011, pp. 576-578.

[6] M. Dahrul, H. Alatas, Irzaman, Preparation and Optical Properties Study of CuO thin Film as Applied Solar Cell on LAPAN-IPB Satellite, Procedia Environmental Sciences, 33 (2016) 661-667.

[7] S. Ahmmed, A. Aktar, S. Tabassum, M.H. Rahman, M.F. Rahman, A.B. Md. Ismail, CuO based solar cell with V2O5 BSF layer: Theoretical validation of experimental data, Superlattices and Microstructures, 151 (2021).

[8] F. Wang, H. Li, Z. Yuan, Y. Sun, F. Chang, H. Deng, L. Xie, H. Li, A highly sensitive gas sensor based on CuO nanoparticles synthetized via a sol–gel method, RSC Advances, 6 (2016) 79343-79349.

[9] M. Hübner, C.E. Simion, A. Tomescu-Stănoiu, S. Pokhrel, N. Bârsan, U. Weimar, Influence of humidity on CO sensing with p-type CuO thick film gas sensors, Sensors and Actuators B: Chemical, 153 (2011) 347-353.

[10] Y.C.a.H.C. Zeng, Controlled Synthesis and Self-Assembly of Single-Crystalline CuO Nanorods and Nanoribbons, CRYSTAL GROWTH & DESIGN, 4 (2004) 397-402.

[11] S.H. JUN WANG, ZHANSHUANG LI, XIAOYAN JING, MILIN ZHANG and ZHAOHUA JIANG, Synthesis of chrysalis-like CuO nanocrystals and their catalytic activity in the thermal decomposition of ammonium perchlorate, J. Chem. Sci.,, 121 (2009) 1077–1081.

[12] T.H. Xuchuan Jiang, and Younan Xia, CuO Nanowires Can Be Synthesized by Heating Copper Substrates in Air, nano letters, 2 (2002) 1333-1338.

[13] P. Raksa, A. Gardchareon, T. Chairuangsri, P. Mangkorntong, N. Mangkorntong, S. Choopun, Ethanol sensing properties of CuO nanowires prepared by an oxidation reaction, Ceramics International, 35 (2009) 649-652.

[14] S. J, P. Priyanka Jain, J. S, Study of Structural and Morphological Properties of Vacuum Coated Copper Oxide (Cuo) Thin Film by Thermal Evaporation Technique, International Journal of Current Research and Review, 10 (2018) 91-93.

[15] H.-L. Chen, T.-H. Chiang, M.-C. Wu, Evolution of Morphology of Nano-Scale CuO Grown on Copper Metal Sheets in 5 wt% NaCl Solution of Spray Fog Environment, Journal of Surface Engineered Materials and Advanced Technology, 02 (2012) 278-283.

[16] Y.H. Ko, G. Nagaraju, S.H. Lee, J.S. Yu, Facile preparation and optoelectronic properties of CuO nanowires for violet light sensing, Materials Letters, 117 (2014) 217-220.

[17] H. Kim, C. Jin, S. Park, S. Kim, C. Lee, H2S gas sensing properties of bare and Pd-functionalized CuO nanorods, Sensors and Actuators B: Chemical, 161 (2012) 594-599.

[18] Y.-S. Kim, I.-S. Hwang, S.-J. Kim, C.-Y. Lee, J.-H. Lee, CuO nanowire gas sensors for air quality

control in automotive cabin, Sensors and Actuators B: Chemical, 135 (2008) 298-303.
[19] C. Wang, X.Q. Fu, X.Y. Xue, Y.G. Wang, T.H. Wang, Surface accumulation conduction controlled sensing characteristic of p-type CuO nanorods induced by oxygen adsorption, Nanotechnology, 18 (2007).
[20] Y. Sun, L. Ma, B. Zhou, P. Gao, Cu(OH)2 and CuO nanotube networks from hexaoxacyclooctadecane-like posnjakite microplates: Synthesis and electrochemical hydrogen storage, International Journal of Hydrogen Energy, 37 (2012) 2336-2343.
[21] K. Khun, Z.H. Ibupoto, M. Willander, Urea Assisted Synthesis of Flower Like CuO Nanostructures and Their Chemical Sensing Application for the Determination of Cadmium Ions, Electroanalysis, 25 (2013) 1425-1432.
[22] A. Das, B. Venkataramana, D. Partheephan, A.K. Prasad, S. Dhara, A.K. Tyagi, Facile synthesis of nanostructured CuO for low temperature NO2 sensing, Physica E: Low-dimensional Systems and Nanostructures, 54 (2013) 40-44.
[23] G.G. Welegergs, R. Akoba, J. Sacky, Z.Y. Nuru, Structural and optical properties of copper oxide (CuO) nanocoatings as selective solar absorber, Materials Today: Proceedings, 36 (2021) 509-513.
[24] A. Taubert, F. Stange, Z. Li, M. Junginger, C. Gunter, M. Neumann, A. Friedrich, CuO Nanoparticles from the strongly hydrated ionic liquid precursor (ILP) tetrabutylammonium hydroxide: evaluation of the ethanol sensing activity, ACS Appl Mater Interfaces, 4 (2012) 791-795.
[25] R.-C.W.a.C.-H. Li, Improved Morphologies and Enhanced Field Emissions of CuO Nanoneedle Arrays by Heating ZnO Coated Copper Foils, CRYSTAL GROWTH & DESIGN, 9 (2009) 2229–2234.
[26] N.K. Hassan, M.R. Hashim, M. Bououdina, Optical properties and I–V characteristics of ZnO nanostructures grown by electrochemical deposition on Si (111) and Si (100), Superlattices and Microstructures, 62 (2013) 182-191.
[27] H. Siddiqui, M.R. Parra, M.S. Qureshi, M.M. Malik, F.Z. Haque, Studies of structural, optical, and electrical properties associated with defects in sodium-doped copper oxide (CuO/Na) nanostructures, Journal of Materials Science, 53 (2018) 8826-8843.
[28] F.M. Fakhree, I.F. Waheed, K.M. Mahmoud, Synthesis and characterization of CuO nanoparticles stabilized by quercetin and its application for anti-breast cancer activity, Egyptian Journal of Chemistry, 0 (2021) 0-0.
[29] H.J. Jung, Y. Yu, M.Y. Choi, Facile Preparation of Cu2O and CuO Nanoparticles by Pulsed Laser Ablation in NaOH Solutions of Different Concentration, Bulletin of the Korean Chemical Society, 36 (2015) 3-4.
[30] Y.-F. Lim, J.J. Choi, T. Hanrath, Facile Synthesis of Colloidal CuO Nanocrystals for Light-Harvesting Applications, Journal of Nanomaterials, 2012 (2012) 1-6.
[31] R. Bunea, A.K. Saikumar, K. Sundaram, A Comparison of Optical Properties of CuO and Cu₂O Thin Films for Solar Cell Applications, Materials Sciences and Applications, 12 (2021) 315-329.
[32] S. Rehman, A. Mumtaz, S.K. Hasanain, Size effects on the magnetic and optical properties of CuO nanoparticles, Journal of Nanoparticle Research, 13 (2010) 2497-2507.
[33] V. Usha, S. Kalyanaraman, R. Thangavel, R. Vettumperumal, Effect of catalysts on the synthesis of CuO nanoparticles: Structural and optical properties by sol–gel method, Superlattices and Microstructures, 86 (2015) 203-210.
[34] G. Chaloeipote, R. Prathumwan, K. Subannajui, A. Wisitsoraat, C. Wongchoosuk, 3D printed CuO semiconducting gas sensor for ammonia detection at room temperature, Materials Science in Semiconductor Processing, 123 (2021).
[35] A.A. Al-Ghamdi, M.H. Khedr, M. Shahnawaze Ansari, P.M.Z. Hasan, M.S. Abdel-wahab, A.A. Farghali, RF sputtered CuO thin films: Structural, optical and photo-catalytic behavior, Physica E: Low-dimensional Systems and Nanostructures, 81 (2016) 83-90.
[36] Y. Du, X. Gao, X. Zhang, X. Meng, Characterization of the microstructure and the optical and electrical properties of the direct-current magnetron sputtered CuO films at different substrate temperatures, Physica B: Condensed Matter, 546 (2018) 28-32.
[37] F. Shao, F. Hernández-Ramírez, J.D. Prades, C. Fàbrega, T. Andreu, J.R. Morante, Copper (II) oxide nanowires for p-type conductometric NH3 sensing, Applied Surface Science, 311 (2014) 177-181.
[38] N. Sharma, N. Sharma, P. Srinivasan, S. Kumar, J.B. Balaguru Rayappan, K. Kailasam, Heptazine based organic framework as a chemiresistive sensor for ammonia detection at room temperature, Journal of Materials Chemistry A, 6 (2018) 18389-18395.
[39] P.L. Rajeev K. Srivastava, R. Dwivedi, SK. Srivastava*, Sensing mechanism in tin oxide-based thick-film gas sensors, Sensors and Actuators B 21 (Sensors and Actuators B 21 (1994) 213-218) 213-218.